Mathematical Biosciences and Engineering

http://www.aimspress.com/journal/mbe

MBE, 20(11): 20093–20115.
DOI: 10.3934/mbe.2023890
Received: 07 September 2023
Revised: 17 October 2023
Accepted: 25 October 2023
Published: 03 November 2023

Research article

Stability and Hopf bifurcation analysis of a fractional-order ring-hub structure neural network with delays under parameters delay feedback control

Yuan Ma and Yunxian Dai*

Department of System Science and Applied Mathematics, Kunming University of Science and Technology, Kunming 650500, China

* **Correspondence:** Email: dyxian1976@sina.com.

Abstract: In this paper, a fractional-order two delays neural network with ring-hub structure is investigated. Firstly, the stability and the existence of Hopf bifurcation of proposed system are obtained by taking the sum of two delays as the bifurcation parameter. Furthermore, a parameters delay feedback controller is introduced to control successfully Hopf bifurcation. The novelty of this paper is that the characteristic equation corresponding to system has two time delays and the parameters depend on one of them. Selecting two time delays as the bifurcation parameters simultaneously, stability switching curves in (τ_1, τ_2) plane and crossing direction are obtained. Sufficient criteria for the stability and the existence of Hopf bifurcation of controlled system are given. Ultimately, numerical simulation shows that parameters delay feedback controller can effectively control Hopf bifurcation of system.

Keywords: fractional-order two-delay neural network; ring-hub structure; Hopf bifurcation; parameters delay feedback control; stability switching curves

1. Introduction

The construction of neural networks in biological system is complex and multifaceted. Inspired by the structure and function of biological neural networks, artificial neural networks have attracted the attention of many scholars and have been applied in many fields, such as disease diagnosis, signal and image processing, associative memory, combinatorial optimization, artificial intelligence and pattern recognition [1–4]. Through further research, scholars have proposed adaptive neural networks [5], feedback neural networks [6], recurrent neural networks [7], cellular neural networks [8] and so on. In addition, due to the different capacities of transmitting, receiving and processing information among different neurons, time delay cannot be ignored for neural networks. Time delay can lead to dynamic behaviors of neural networks with poor performance, oscillation, bifurcation and chaos [9, 10]. It is known that Hopf bifurcation phenomenon is universal in the neural networks [11,12]. Considering that modeling work involving biological or physical processes takes time to complete, multiple time delays occur naturally [13,14].

In recent years, fractional calculus has been widely used in engineering mathematics, physics, biology and economics because of its genetic and wireless storage properties [15–18]. Based on this property, fractional integration operator is introduced into neural network systems. Researches have shown that fractional-order systems can more accurately represent memory features compared to integer-order systems, thereby enabling the ability of neurons to effectively transmit and process information. Therefore, fractional-order neural network systems have gained widespread attention. Huang et al. [19] discussed fractional order-induced bifurcations in a delayed neural network with three neurons. Xu et al. [20] investigated Hopf bifurcation on simplified BAM neural networks with multiple delays. In [21], a fractional-order recurrent neural network is proposed and the stability and Hopf bifurcation are investigated.

Although there have been many studies on bifurcation of fractional-order neural networks, most of them only consider neural networks with a single structure. In general, the structure of neural networks can be divided into ring structure, star structure, linked structure, and hub structure. In view of the diversity and complexity of real neural networks, the impact of network topology on the dynamic behavior of the network cannot be ignored. Tao et al. [22] put forward a bidirectional super-ring-shaped delayed neural network polymer with n neurons and investigated the influence of time delay on the dynamics of the network. In [23], a class of $4n$-dimensional delayed neural networks with radial-ring configuration and bidirectional coupling is proposed. Further research shows that neural networks with hub structure are beneficial to information integration. In addition, the ring structure of the network can effectively solve the congestion problem caused by the increase of information traffic. Based on the characteristics of the two structures, Chen et al. [24] studied the stability and Hopf bifurcation of a high-dimensional fractional delayed neural network containing a ring-hub structure. In order to achieve better performance of neural networks, inspired by [24], this paper considers the following a fractional-order 4-neuron ring-hub structure neural network with two time delays:

$$\begin{cases} D^{\theta}x_1(t) = -\sigma x_1(t) + c_{31}f(x_3(t)) + c_{41}f(x_4(t-\tau_2)), \\ D^{\theta}x_2(t) = -\sigma x_2(t) + c_{12}f(x_1(t)) + c_{42}f(x_4(t-\tau_2)), \\ D^{\theta}x_3(t) = -\sigma x_3(t) + c_{23}f(x_2(t)) + c_{43}f(x_4(t-\tau_2)), \\ D^{\theta}x_4(t) = -\sigma x_4(t) + c_{14}f(x_1(t-\tau_1)) + c_{24}f(x_2(t-\tau_1)) + c_{34}f(x_3(t-\tau_1)), \end{cases} \tag{1.1}$$

where $\theta \in (0,1]$ is the fractional order, D^{θ} denotes the Caputo fractional derivative; $x_i(t)(i = 1,2,3,4)$ denotes the state variable of the ith neuron at time t; $\sigma > 0$ describes the internal decay rate of neurons; $c_{ij}(i, j = 1,2,3,4)$ stands for the connection weight from the ith neuron to the jth neuron; f represents the activation function; $\tau_2 \geq 0$ is the time delay of signal transmission from central neuron $x_4(t)$ to peripheral neuron $x_i(t)(i = 1,2,3)$; conversely, the time delay of signal transmission from peripheral neuron to central neuron is $\tau_1 \geq 0$. The initial conditions of system (1.1) are $x_i(\xi) = \phi_i(\xi), \phi_i(\xi) \geq 0, i = 1,2,3,4, -\sigma \leq \xi \leq 0, \sigma = max\{\tau_1, \tau_2\}$. Throughout this paper, we make the following assumption:

$(H1)$ $\quad f \in C^1, f(0) = 0, f'(0) \neq 0.$

In the fields of biology, economy, fluid dynamics and communication security, the transmission delay of a signal often affects the overall response of system. Considering that bifurcation caused by time delay may be harmful, a controller is introduced to control the bifurcation phenomena. Bifurcation control generally involves delaying the occurrence of inherent bifurcation, modifying the critical value of existing bifurcation point, and stabilizing the bifurcation solutions or branches. There are various methods of bifurcation control. For instance, Ma et al. [25] investigated a parametric delay feedback controller on van der Pol–Duffing oscillator, which makes the coefficients of the system dependent on time delay. In [26], a hybrid control strategy is proposed and the existence of Hopf bifurcation with time-delays Hopfield neural network is analyzed. A delayed feedback controller [27] is used for Hopf bifurcation control of small-world network model. In order to achieve optimal dynamic behaviors, the controller proposed in [27] is implemented in this paper, and the following parameters delay feedback control of ring-hub structure neural network is considered

$$\begin{cases} D^{\theta}x_1(t) = -\sigma x_1(t) + c_{31}f(x_3(t)) + c_{41}f(x_4(t-\tau_2)), \\ D^{\theta}x_2(t) = -\sigma x_2(t) + c_{12}f(x_1(t)) + c_{42}f(x_4(t-\tau_2)), \\ D^{\theta}x_3(t) = -\sigma x_3(t) + c_{23}f(x_2(t)) + c_{43}f(x_4(t-\tau_2)), \\ D^{\theta}x_4(t) = -\sigma x_4(t) + c_{14}f(x_1(t-\tau_1)) + c_{24}f(x_2(t-\tau_1)) + c_{34}f(x_3(t-\tau_1)) + ke^{-P(\tau_1)}x_4(t-\tau_1), \end{cases} \tag{1.2}$$

where $ke^{-P(\tau_1)}$ is parameters delay feedback controller. Let $P(\tau_1) = p\tau_1$, p is called the decay rate. Note that the feedback controller $ke^{-p\tau_1}$ is a function that decreases exponentially with time delay. This means that the feedback effect of past states diminishes with time t.

For systems with two delays and delay dependent parameters, the method of stability switching curves is proposed to study the dynamic behaviors of system. In [28], a class of integer-order two delays models with delay dependent parameters is considered. The corresponding characteristic equation has the following form

$$P_0(\lambda,\tau) + P_1(\lambda,\tau)e^{-\lambda\tau} + P_2(\lambda,\tau)e^{-\lambda\tau_1} = 0, \tag{1.3}$$

where $P_i(\lambda,\tau), i = 0, 1, 2$ are polynomials in λ and P_i only depend on τ. Authors proposed a geometric method to study Eq (1.3), which obtains the stability switching curves in the whole two time delays parameter plane. The direction of bifurcation in stability switching curves is determined according to the direction of the characteristic roots crossing the imaginary axis. The stability condition of system at the equilibrium point is obtained. This method is applied to study the effect of two delays on stability of an HIV infection model [29] and a planktonic resource-consumer system [30]. In addition, the geometric method [28] is also applicable to the characteristic equation with the form of

$$P_0(\lambda,\tau) + P_1(\lambda,\tau)e^{-\lambda\tau} + P_2(\lambda,\tau)e^{-\lambda(\tau+\tau_1)} = 0. \tag{1.4}$$

There are few papers discussing the stability of neural networks with multiple time delays changing simultaneously and delay dependent parameters. In this paper, the method of stability switching curves is first used to discuss the stability and the existence of Hopf bifurcation of a fractional-order neural network with a composite ring-hub structure with two time delays changing simultaneously and delay dependent parameters. The main contribution of this paper are as follows:

(i) Considering the complex topology of neural networks, a fractional-order two time delays neural network with a composite ring-hub structure is considered.

(ii) By taking the time delay as the bifurcation parameter, sufficient conditions for the stability and the existence of Hopf bifurcation are established. The research results show that delays and the fractional-order can affect the stability of system.

(iii) A parameters delay feedback controller is introduced into the fractional-order neural network system with a composite ring-hub structure, and controls successfully Hopf bifurcation.

(iv) It is the first time to apply the method of stability switching curves to a fractional-order neural network system. The influence of time delays changing simultaneously on the stability of fractional-order controlled system (1.2) is analyzed.

The rest of this paper is organized as follows: In Section 2, we consider the local stability and the existence of Hopf bifurcation of system (1.1). In Section 3, the parameters delay feedback controller is introduced into system (1.1). The stability and existence of Hopf bifurcation of system (1.2) are discussed by using the method of stability switching curves. In Section 4, numerical simulation is adopted to verify the correctness of theoretical results. Finally, the conclusions are given in Section 5.

2. Stability and Hopf bifurcation analysis of system (1.1)

In this section, $\tau = \tau_1 + \tau_2$ is selected as the bifurcation parameter to study the local stability of the equilibrium and the existence of Hopf bifurcation of system (1.1). Based on assumption $(H1)$, it can be concluded that the equilibrium of system (1.1) is the origin $O(0, 0, 0, 0)$. The corresponding linear system of system (1.1) at O is

$$\begin{cases} D^{\theta}x_1(t) = -\sigma x_1(t) + \varphi_{31}x_3(t) + \varphi_{41}x_4(t-\tau_2), \\ D^{\theta}x_2(t) = -\sigma x_2(t) + \varphi_{12}x_1(t) + \varphi_{42}x_4(t-\tau_2), \\ D^{\theta}x_3(t) = -\sigma x_3(t) + \varphi_{23}x_2(t) + \varphi_{43}x_4(t-\tau_2), \\ D^{\theta}x_4(t) = -\sigma x_4(t) + \varphi_{14}x_1(t-\tau_1) + \varphi_{24}x_2(t-\tau_1) + \varphi_{34}x_3(t-\tau_1), \end{cases} \tag{2.1}$$

where $\varphi_{ij} = c_{ij}f'(0)(i, j = 1, 2, 3, 4)$.

By applying Laplace transformation, the characteristic equation of system (2.1) is

$$\begin{vmatrix} s^{\theta}+\sigma & 0 & -\varphi_{31} & -\varphi_{41}e^{-s\tau_2} \\ -\varphi_{12} & s^{\theta}+\sigma & 0 & -\varphi_{42}e^{-s\tau_2} \\ 0 & -\varphi_{23} & s^{\theta}+\sigma & -\varphi_{43}e^{-s\tau_2} \\ -\varphi_{14}e^{-s\tau_1} & -\varphi_{24}e^{-s\tau_1} & -\varphi_{34}e^{-s\tau_1} & s^{\theta}+\sigma \end{vmatrix} = 0, \tag{2.2}$$

that is

$$s^{4\theta} + q_1 s^{3\theta} + q_2 s^{2\theta} + q_3 s^{\theta} + q_4 + (q_5 s^{2\theta} + q_6 s^{\theta} + q_7)e^{-s(\tau_1+\tau_2)} = 0, \tag{2.3}$$

where

$$\begin{aligned} &q_1 = 4\sigma, \quad q_2 = 6\sigma^2, \quad q_3 = 4\sigma^3 - \varphi_{12}\varphi_{23}\varphi_{31}, \quad q_4 = \sigma^4 - \varphi_{12}\varphi_{23}\varphi_{31}\sigma, \\ &q_5 = -\varphi_{14}\varphi_{41} - \varphi_{24}\varphi_{42} - \varphi_{34}\varphi_{43}, \\ &q_6 = 2\sigma q_5 - \varphi_{23}\varphi_{34}\varphi_{42} - \varphi_{12}\varphi_{24}\varphi_{41} - \varphi_{14}\varphi_{31}\varphi_{43}, \\ &q_7 = q_5\sigma^2 - \sigma(\varphi_{23}\varphi_{34}\varphi_{42} + \varphi_{12}\varphi_{24}\varphi_{41} + \varphi_{14}\varphi_{31}\varphi_{43}) - \varphi_{12}\varphi_{24}\varphi_{31}\varphi_{43} \\ &\qquad - \varphi_{12}\varphi_{23}\varphi_{34}\varphi_{41} - \varphi_{14}\varphi_{23}\varphi_{31}\varphi_{42}. \end{aligned}$$

The stability of the equilibrium O is discussed in two scenarios.

Case I: $\tau_1 = \tau_2 = 0$.

If $\tau_1 = \tau_2 = 0$, Equation (2.3) becomes

$$s^{4\theta} + b_1 s^{3\theta} + b_2 s^{2\theta} + b_3 s^{\theta} + b_4 = 0, \tag{2.4}$$

where

$$b_1 = q_1, \quad b_2 = q_2 + q_5, \quad b_3 = q_3 + q_6, \quad b_4 = q_4 + q_7.$$

Lemma 2.1. *[31] For the following fractional-order system: $D^{\theta}x(t) = Ax(t), A \in R^{n\times n}$, the equilibrium of system is locally asymptotically stable if and only if all the eigenvalues $s_i (i = 1, 2, \ldots, n)$ of A satisfy $|arg(s_i)| > \theta\pi/2$, where $\theta \in (0, 1]$.*

According to Lemma 2.1 and Routh-Hurwitz criterion, we have the following theorem.

Theorem 2.1. *System* (1.1) *is locally asymptotically stable if and only if $D_i > 0 (i = 1, 2, 3, 4)$ holds, where D_i is defined as follows*

$$D_1 = b_1, D_2 = \begin{vmatrix} b_1 & 1 \\ b_3 & b_2 \end{vmatrix}, D_3 = \begin{vmatrix} b_1 & 1 & 0 \\ b_3 & b_2 & b_1 \\ 0 & b_4 & b_3 \end{vmatrix}, D_4 = b_4 D_3 > 0.$$

Proof. If $D_i > 0 (i = 1, 2, 3, 4)$ holds, we can conclude that all the roots s_i satisfy $|arg(s_i)| > \theta\pi/2 (i = 1, 2, 3, 4)$. It follows from Lemma 2.1 that system (1.1) with $\tau_1 = \tau_2 = 0$ is locally asymptotically stable.

Case II: $\tau_1 > 0, \tau_2 > 0$.
Let $\tau = \tau_1 + \tau_2$, Equation (2.3) becomes

$$Q(s, \tau) = Q_0(s) + Q_1(s)e^{-s\tau} = 0, \tag{2.5}$$

where

$$\begin{aligned} Q_0(s) &= s^{4\theta} + q_1 s^{3\theta} + q_2 s^{2\theta} + q_3 s^{\theta} + q_4, \\ Q_1(s) &= q_5 s^{2\theta} + q_6 s^{\theta} + q_7. \end{aligned}$$

Assuming that the characteristic equation (2.5) has a purely imaginary root $s = \omega(\cos\frac{\pi}{2} + i\sin\frac{\pi}{2})(\omega > 0)$. Substituting s into Eq (2.5) and separating real and imaginary parts, we get

$$\begin{cases} Q_0^r + Q_1^r \cos\omega\tau + Q_1^i \sin\omega\tau = 0, \\ Q_0^i + Q_1^i \cos\omega\tau - Q_1^r \sin\omega\tau = 0, \end{cases} \tag{2.6}$$

where

$$\begin{aligned} Q_0^r &= \omega^{4\theta}\cos 2\theta\pi + q_1\omega^{3\theta}\cos\frac{3\theta\pi}{2} + q_2\omega^{2\theta}\cos\theta\pi + q_3\omega^{\theta}\cos\frac{\theta\pi}{2} + q_4, \\ Q_0^i &= \omega^{4\theta}\sin 2\theta\pi + q_1\omega^{3\theta}\sin\frac{3\theta\pi}{2} + q_2\omega^{2\theta}\sin\theta\pi + q_3\omega^{\theta}\sin\frac{\theta\pi}{2}, \\ Q_1^r &= q_5\omega^{2\theta}\cos\theta\pi + q_6\omega^{\theta}\cos\frac{\theta\pi}{2} + q_7, \quad Q_1^i = q_5\omega^{2\theta}\sin\theta\pi + q_6\omega^{\theta}\sin\frac{\theta\pi}{2}. \end{aligned}$$

By calculation, one obtains

$$\begin{aligned} \cos\omega\tau &= -\frac{Q_0^r Q_1^r + Q_0^i Q_1^i}{Q_1^{r2} + Q_1^{i2}}, \\ \sin\omega\tau &= \frac{Q_0^i Q_1^r - Q_0^r Q_1^i}{Q_1^{r2} + Q_1^{i2}}. \end{aligned} \tag{2.7}$$

Since $\cos^2\omega\tau + \sin^2\omega\tau = 1$, we can obtain

$$\omega^{8\theta} + c_1\omega^{7\theta} + c_2\omega^{6\theta} + c_3\omega^{5\theta} + c_4\omega^{4\theta} + c_5\omega^{3\theta} + c_6\omega^{2\theta} + c_7\omega^{\theta} + c_8 = 0, \tag{2.8}$$

where

$$\begin{aligned} &c_1 = 2q_1\cos\frac{\theta\pi}{2}, \quad c_2 = q_1^2 + 2q_2\cos\theta\pi, \quad c_3 = 2q_3\cos\frac{3\theta\pi}{2} + 2q_1q_2\cos\frac{\theta\pi}{2}, \\ &c_4 = q_2^2 + 2q_4\cos 2\theta\pi + 2q_1q_3\cos\theta\pi - q_5^2, \quad c_5 = 2q_1q_4\cos\frac{3\theta\pi}{2} + 2(q_2q_3 - q_5q_6)\cos\frac{\theta\pi}{2}, \\ &c_6 = q_3^2 - q_6^2 + 2(q_2q_4 - q_5q_7)\cos\theta\pi, \quad c_7 = 2(q_3q_4 - q_6q_7)\cos\frac{\theta\pi}{2}, \quad c_8 = q_4^2 - q_7^2. \end{aligned}$$

Let

$$F(\omega) = \omega^{8\theta} + c_1\omega^{7\theta} + c_2\omega^{6\theta} + c_3\omega^{5\theta} + c_4\omega^{4\theta} + c_5\omega^{3\theta} + c_6\omega^{2\theta} + c_7\omega^{\theta} + c_8.$$

To obtain the main results, we make the following assumption:

$$(H2) \quad c_8 < 0,$$

then $\lim_{\omega\to\infty} F(\omega) = +\infty$ and Eq (2.8) has at least one positive root ω_i. According to Eq (2.7), we have

$$\tau_i^{(k)} = \frac{1}{\omega_i}[\arccos(-\frac{Q_0^r Q_1^r + Q_0^i Q_1^i}{|Q_1^{r2} + Q_1^{i2}|}) + 2j\pi], j = 0, 1, 2, \cdots . \tag{2.9}$$

Denote

$$\tau_0 = \tau_{i_0}^{(0)} = \min_{i=1,2,\cdots}\left\{\tau_i^{(0)}\right\}, \omega_0 = \omega_{i_0}. \tag{2.10}$$

There exists a simple pair of purely imaginary roots for Eq (2.5) when $\tau = \tau_0$, and all roots of Eq (2.5) for $\tau \in (0, \tau_0)$ have strictly negative real parts. Let $s(\tau) = \mu(\tau) + i\omega(\tau)(\omega > 0)$ be the root of Eq (2.5) near $\tau = \tau_i^{(k)}$ complying with $\mu(\tau_i^{(k)}) = 0, \omega(\tau_i^{(k)}) = \omega_i$. Substituting $s(\tau)$ into Eq (2.5) and taking the derivative of s with respect to τ, one gets

$$\frac{\mathrm{d}s}{\mathrm{d}\tau} = \frac{\Phi(s)}{\Psi(s)}, \tag{2.11}$$

where

$$\begin{aligned} \Phi(s) &= se^{-s\tau}(q_5s^{2\theta} + q_6s^{\theta} + q_7), \\ \Psi(s) &= 4\theta s^{4\theta-1} + 3\theta q_1 s^{3\theta-1} + 2\theta q_2 s^{2\theta-1} + \theta q_3 s^{\theta-1} + \left[2\theta q_5 s^{2\theta-1} + \theta q_6 s^{\theta-1} - \tau(q_5s^{2\theta} + q_6s^{\theta} + q_7)\right]e^{-s\tau}. \end{aligned}$$

It follows from Eq (2.11)

$$Re\left[\frac{\mathrm{d}s}{\mathrm{d}\tau}\right]\Big|_{\tau=\tau_i^{(k)}} = \frac{\Phi_1\Psi_1+\Phi_2\Psi_2}{\Psi_1^2+\Psi_2^2},$$

where

$$\begin{aligned}
\Phi_1 &= q_5\omega_i^{2\theta+1}\sin(\omega_i\tau_i^{(k)}-\theta\pi)+q_6\omega_i^{\theta+1}\sin(\omega_i\tau_i^{(k)}-\frac{\theta\pi}{2})+q_7\omega_i\sin\omega_i\tau_i^{(k)},\\
\Phi_2 &= q_5\omega_i^{2\theta+1}\cos(\omega_i\tau_i^{(k)}-\theta\pi)+q_6\omega_i^{\theta+1}\cos(\omega_i\tau_i^{(k)}-\frac{\theta\pi}{2})+q_7\omega_i\cos\omega_i\tau_i^{(k)},\\
\Psi_1 &= 4\theta\omega_i^{4\theta-1}\sin 2\theta\pi+3\theta q_1\omega_i^{3\theta-1}\sin\frac{3\theta\pi}{2}-\tau_i^{(k)}q_5\omega_i^{2\theta}\cos(\omega_i\tau_i^{(k)}-\theta\pi)\\
&\quad+2\theta\omega_i^{2\theta-1}[q_2\sin\theta\pi-q_5\sin(\omega_i\tau_i^{(k)}-\theta\pi)]-\tau_i^{(k)}q_6\omega_i^{\theta}\cos(\omega_i\tau_i^{(k)}-\frac{\theta\pi}{2})\\
&\quad+\theta\omega_i^{\theta-1}[q_3\sin\frac{\theta\pi}{2}-q_6\sin(\omega_i\tau_i^{(k)}-\frac{\theta\pi}{2})]-\tau_i^{(k)}q_7\cos\omega_i\tau_i^{(k)},\\
\Psi_2 &= -4\theta\omega_i^{4\theta-1}\cos 2\theta\pi-3\theta q_1\omega_i^{3\theta-1}\cos\frac{3\theta\pi}{2}+\tau_i^{(k)}q_5\omega_i^{2\theta}\sin(\omega_i\tau_i^{(k)}-\theta\pi)\\
&\quad-2\theta\omega_i^{2\theta-1}[q_2\cos\theta\pi+q_5\cos(\omega_i\tau_i^{(k)}-\theta\pi)]+\tau_i^{(k)}q_6\omega_i^{\theta}\sin(\omega_i\tau_i^{(k)}-\frac{\theta\pi}{2})\\
&\quad-\theta\omega_i^{\theta-1}[q_3\cos\frac{\theta\pi}{2}+q_6\cos(\omega_i\tau_i^{(k)}-\frac{\theta\pi}{2})]+\tau_i^{(k)}q_7\sin\omega_i\tau_i^{(k)}.
\end{aligned}$$

Due to $\Psi_1^2+\Psi_2^2>0$, we have

$$sign\left\{Re\left[\frac{\mathrm{d}s}{\mathrm{d}\tau}\right]\Big|_{\tau=\tau_i^{(k)}}\right\} = sign\left\{\Phi_1\Psi_1+\Phi_2\Psi_2\right\}. \tag{2.12}$$

If assumption

$$(H3)\quad \Phi_1\Psi_1+\Phi_2\Psi_2\neq 0,$$

is holds, then the transversality condition $Re\left[\frac{\mathrm{d}s}{\mathrm{d}\tau}\right]|_{\tau=\tau_i^{(k)}}\neq 0$ holds.

Based on the above analysis, the following theorem can be obtained.

Theorem 2.2. *For system* (1.1)*, assumptions* $(H1)-(H3)$ *hold.*

(i) *If* $\tau\in[0,\tau_0)$*, then the equilibrium O is locally asymptotically stable;*

(ii) *If* $\tau>\tau_0$*, then system* (1.1) *undergoes Hopf bifurcation at O when* $\tau=\tau_0$.

3. Stability and Hopf bifurcation analysis of system (1.2)

In this section, we introduce the parameters delay feedback controller into system (1.1). The stability and the existence of Hopf bifurcation of system (1.2) are studied by applying the method of stability switching curves.

The linearized system (1.2) at equilibrium $O(0,0,0,0)$ is given by

$$\begin{cases}
D^{\theta}x_1(t) = -\sigma x_1(t)+\varphi_{31}x_3(t)+\varphi_{41}x_4(t-\tau_2),\\
D^{\theta}x_2(t) = -\sigma x_2(t)+\varphi_{12}x_1(t)+\varphi_{42}x_4(t-\tau_2),\\
D^{\theta}x_3(t) = -\sigma x_3(t)+\varphi_{23}x_2(t)+\varphi_{43}x_4(t-\tau_2),\\
D^{\theta}x_4(t) = -\sigma x_4(t)+\varphi_{14}x_1(t-\tau_1)+\varphi_{24}x_2(t-\tau_1)+\varphi_{34}x_3(t-\tau_1)+ke^{-P(\tau_1)}x_4(t-\tau_1).
\end{cases} \tag{3.1}$$

The characteristic equation corresponding to system (3.1) can be obtained

$$D(s,\tau_1,\tau_2) = P_0(s,\tau_1) + P_1(s,\tau_1)e^{-s\tau_1} + P_2(s,\tau_1)e^{-s(\tau_1+\tau_2)}, \tag{3.2}$$

where

$$\begin{aligned}
&P_0(s,\tau_1) = s^{4\theta} + 4\sigma s^{3\theta} + 6\sigma^2 s^{2\theta} + A_1 s^{\theta} + A_2,\\
&P_1(s,\tau_1) = -e^{-p\tau_1}(ks^{3\theta} + 3k\sigma s^{2\theta} + A_3 s^{\theta} + A_4),\\
&P_2(s,\tau_1) = A_5 s^{2\theta} + A_6 s^{\theta} + A_7,\\
&A_1 = 4\sigma^3 - \varphi_{12}\varphi_{23}\varphi_{31}, \quad A_2 = \sigma^4 - \sigma\varphi_{12}\varphi_{23}\varphi_{31}, \quad A_3 = 3k\sigma^2, \quad A_4 = k\sigma^3 + k\varphi_{12}\varphi_{23}\varphi_{31},\\
&A_5 = -\varphi_{14}\varphi_{41} - \varphi_{24}\varphi_{42} - \varphi_{34}\varphi_{43}, \quad A_6 = 2\sigma A_5 - \varphi_{23}\varphi_{34}\varphi_{42} - \varphi_{12}\varphi_{24}\varphi_{41} - \varphi_{14}\varphi_{31}\varphi_{43},\\
&A_7 = A_5\sigma^2 - \sigma(\varphi_{23}\varphi_{34}\varphi_{42} + \varphi_{12}\varphi_{24}\varphi_{41} + \varphi_{14}\varphi_{31}\varphi_{43}) - \varphi_{12}\varphi_{24}\varphi_{31}\varphi_{43} - \varphi_{12}\varphi_{23}\varphi_{34}\varphi_{41} - \varphi_{14}\varphi_{23}\varphi_{31}\varphi_{42}.
\end{aligned}$$

When $\tau_1 = \tau_2 = 0$, the characteristic equation (3.2) reduces to

$$s^{4\theta} + B_1 s^{3\theta} + B_2 s^{2\theta} + B_3 s^{\theta} + B_4 = 0, \tag{3.3}$$

where

$$B_1 = 4\sigma - k, \quad B_2 = 6\sigma^2 - 3k\sigma + A_5, \quad B_3 = A_1 - A_3 + A_6, \quad B_4 = A_2 - A_4 + A_7.$$

In order to obtain the main result, we assume

$$(H4) \quad B_4(B_1B_2B_3 - B_1^2B_4 - B_3^2) > 0.$$

According the Routh-Hurwitz criterion and Lemma 2.1, we present the following theorem.

Theorem 3.1. *For $\tau_1 = \tau_2 = 0$, if $(H1)$ and $(H4)$ hold, then the equilibrium O of system* (1.2) *is locally asymptotically stable.*

3.1. Stability switching curves

In this subsection, when $\tau_1 > 0, \tau_2 > 0$, and $\tau_1 \neq \tau_2$, the characteristic equation (3.2) with two time delays and one-delay dependent coefficients is discussed using the method in [28]. We firstly give the following basic assumptions:

(i) Existence of a principal term: $deg(P_0(s,\tau_1)) \geq max\{deg(P_1(s,\tau_1)), deg(P_2(s,\tau_1))\}$.

(ii) No zero frequency: $s = 0$ is not a characteristic root for any $\tau_1 \in I$, i.e.,

$$P_0(0,\tau_1) + P_1(0,\tau_1) + P_2(0,\tau_1) \neq 0.$$

(iii) The polynomials $P_l(s,\tau_1), l = 0,1,2$ have no common factor.

(iv) No large oscillation: $\lim\limits_{\substack{Res\geq 0\\ |s|\to\infty}} \sup\limits_{\tau_1\in I}\left(\left|\frac{P_1(s,\tau_1)}{P_0(s,\tau_1)}\right| + \left|\frac{P_2(s,\tau_1)}{P_0(s,\tau_1)}\right|\right) < 1$.

(v) $P_l(i\omega,\tau_1) \neq 0, l = 0,1,2$ for any $\tau_1 \in I$ and $\omega \in \mathbb{R}_+$.

(vi) For any $\omega \in \mathbb{R}_+$, at least one of $|P_l(i\omega,\tau_1)|, l = 0,1,2$ tends to ∞ as $\tau_1 \to -\infty$. If there are multiple such P_l, then these functions tend to infinity at different rates.

Next, we verify that the above assumptions (i)–(vi) hold for Eq (3.2).

For $P_0(s,\tau_1), P_1(s,\tau_1), P_2(s,\tau_1)$, (i) is automatically satisfied.

Due to $P_0(0,\tau_1)+P_1(0,\tau_1)+P_2(0,\tau_1) = A_2 - e^{-p\tau_1}A_4 + A_7 \neq 0$, (ii) is true.

If (iii) does not hold, then there exists a common factor $c(s,\tau_1)$ for $P_l(s,\tau_1), l = 0,1,2$, which causes Eq (3.2) to be decomposed into the product of another transcendental equation satisfying (iii) and $c(s,\tau_1)$.

Since

$$\lim_{\substack{Res\geq 0\\ |s|\to\infty}} \sup_{\tau_1\in I}\left(\left|\frac{-e^{-p\tau_1}(ks^{3\theta}+3k\sigma s^{2\theta}+A_3s^{\theta}+A_4)}{s^{4\theta}+4\sigma s^{3\theta}+6\sigma^2 s^{2\theta}+A_1s^{\theta}+A_2}\right| + \left|\frac{A_5s^{2\theta}+A_6s^{\theta}+A_7}{s^{4\theta}+4\sigma s^{3\theta}+6\sigma^2 s^{2\theta}+A_1s^{\theta}+A_2}\right|\right) = 0 < 1,$$

the condition (iv) holds.

According to the expression for $P_l(s,\tau_1), l = 0,1,2$, (v) is naturally true. The presentation of assumption (vi) helps to reduce the cases of graph for $S_n^{\pm}(\omega,\tau_1)$.

Assume that $s = \omega(\cos\frac{\pi}{2} + i\sin\frac{\pi}{2})(\omega > 0)$ is a pure imaginary root of $D(s,\tau_1,\tau_2) = 0$. Substituting it into Eq (3.2), we get

$$D(\omega,\tau_1,\tau_2) = 1 + a_1(\omega,\tau_1)e^{-i\omega\tau_1} + a_2(\omega,\tau_1)e^{-i\omega(\tau_1+\tau_2)} = 0, \tag{3.4}$$

where

$$a_l(\omega,\tau_1) = P_l(i\omega,\tau_1)/P_0(i\omega,\tau_1), \quad l = 1,2. \tag{3.5}$$

We know that $s = \omega(\cos\frac{\pi}{2} + i\sin\frac{\pi}{2})(\omega > 0)$ is the root of Eq (3.2) if and only if the right side of Eq (3.4) must form a triangle on the complex plane. Based on the relationship between the three sides of the triangle, for some $(\tau_1,\tau_2) \in I \times \mathbb{R}_+$, then (ω,τ_1) satisfies

$$\begin{aligned} &|a_1(\omega,\tau_1)| + |a_2(\omega,\tau_1)| \geq 1,\\ &|a_1(\omega,\tau_1)| - |a_2(\omega,\tau_1)| \leq 1,\\ &|a_2(\omega,\tau_1)| - |a_1(\omega,\tau_1)| \leq 1. \end{aligned} \tag{3.6}$$

Inequalities (3.6) are equivalent to

$$\begin{aligned} F_1(\omega,\tau_1) &:= |P_1(i\omega,\tau_1)| + |P_2(i\omega,\tau_1)| - |P_0(i\omega,\tau_1)| \geq 0,\\ F_2(\omega,\tau_1) &:= |P_0(i\omega,\tau_1)| + |P_2(i\omega,\tau_1)| - |P_1(i\omega,\tau_1)| \geq 0,\\ F_3(\omega,\tau_1) &:= |P_0(i\omega,\tau_1)| + |P_1(i\omega,\tau_1)| - |P_2(i\omega,\tau_1)| \geq 0. \end{aligned} \tag{3.7}$$

The feasible region $\Omega = \{(\omega,\tau_1) \in I \times \mathbb{R}_+ : F_i(\omega,\tau_1) \geq 0, i = 1,2,3\}$, defined by inequalities (3.6) or (3.7) for (ω,τ_1), is such that the characteristic equation (3.2) may have solutions for $\tau_2 \in \mathbb{R}_+$. As discussed in [28], for each connected region Ω_k of Ω, we define the admissible range for ω as $I_k = [\omega_k^l, \omega_k^r], k = 1,2,\cdots,N$. For each $\omega \in I_k$, there exists τ_1-intervals $I_\omega^k = [\tau_{1,\omega}^{k,l}, \tau_{1,\omega}^{k,r}]$ such that Eqs (3.6) or (3.7) holds.

Let $\theta_1(\omega,\tau_1), \theta_2(\omega,\tau_1)$ be the angles formed by 1 and $a_1(\omega,\tau_1)e^{-s\tau_1}$, 1 and $a_2(\omega,\tau_1)e^{-s(\tau_1+\tau_2)}$, respectively. According to the law of cosine, we obtain

$$\theta_1(\omega,\tau_1) = \arccos\left(\frac{1+|a_1(\omega,\tau_1)|^2 - |a_2(\omega,\tau_1)|^2}{2\,|a_1(\omega,\tau_1)|}\right), \tag{3.8}$$

$$\theta_2(\omega,\tau_1) = \arccos\left(\frac{1+|a_2(\omega,\tau_1)|^2 - |a_1(\omega,\tau_1)|^2}{2\,|a_2(\omega,\tau_1)|}\right). \tag{3.9}$$

In the following, two possible cases are considered.

1) If $Im(a_1(\omega,\tau_1)e^{-i\omega\tau_1}) > 0$, we obtain

$$\arg(a_1(\omega,\tau_1)e^{-i\omega\tau_1}) = \pi - \theta_1(\omega,\tau_1), \quad \arg(a_2(\omega,\tau_1)e^{-i\omega(\tau_1+\tau_2)}) = \theta_2(\omega,\tau_1) - \pi,$$

therefore

$$\arg(a_1(\omega,\tau_1)) - \omega\tau_1 + 2n\pi = \pi - \theta_1(\omega,\tau_1), \quad n \in \mathbb{Z}, \tag{3.10}$$

and

$$\arg(a_2(\omega,\tau_1)) - \omega(\tau_1+\tau_2) + 2j\pi = \theta_2(\omega,\tau_1) - \pi, \quad j \in \mathbb{Z}. \tag{3.11}$$

It follows from Eqs (3.10) and (3.11) that

$$\tau_1 = \frac{1}{\omega}[\arg(a_1(\omega,\tau_1)) + \theta_1(\omega,\tau_1) + (2n-1)\pi], \quad n \in \mathbb{Z}, \tag{3.12}$$

and

$$\tau_2 = \frac{1}{\omega}[\arg(a_2(\omega,\tau_1)) - \omega\tau_1 - \theta_2(\omega,\tau_1) + (2j+1)\pi], \quad j \in \mathbb{Z}. \tag{3.13}$$

2) If $Im(a_1(\omega,\tau_1)e^{-i\omega\tau_1}) < 0$, then

$$\arg(a_1(\omega,\tau_1)e^{-i\omega\tau_1}) = \pi + \theta_1(\omega,\tau_1), \quad \arg(a_2(\omega,\tau_1)e^{-i\omega(\tau_1+\tau_2)}) = -\theta_2(\omega,\tau_1) - \pi,$$

therefore

$$\arg(a_1(\omega,\tau_1)) - \omega\tau_1 + 2n\pi = \pi + \theta_1(\omega,\tau_1), \quad n \in \mathbb{Z}, \tag{3.14}$$

and

$$\arg(a_2(\omega,\tau_1)) - \omega(\tau_1+\tau_2) + 2j\pi = -\theta_2(\omega,\tau_1) - \pi, \quad j \in \mathbb{Z}. \tag{3.15}$$

Similarly, according to Eqs (3.14) and (3.15), we get

$$\tau_1 = \frac{1}{\omega}[\arg(a_1(\omega,\tau_1)) - \theta_1(\omega,\tau_1) + (2n-1)\pi], \quad n \in \mathbb{Z}, \tag{3.16}$$

and

$$\tau_2 = \frac{1}{\omega}[\arg(a_2(\omega,\tau_1)) - \omega\tau_1 + \theta_2(\omega,\tau_1) + (2j+1)\pi], \quad j \in \mathbb{Z}. \tag{3.17}$$

Once the values of (ω,τ_1) satisfying Eqs (3.12) or (3.16) are determined, then the critical values of τ_2 are obtained according to Eqs (3.13) or (3.17). Now we define the function $S_n^{\pm} : \Omega \to \mathbb{R}$

$$S_n^{\pm}(\omega,\tau_1) = \tau_1 - \frac{1}{\omega}[\arg(a_1(\omega,\tau_1)) \pm \theta_1(\omega,\tau_1) + (2n-1)\pi], \quad n \in \mathbb{Z}. \tag{3.18}$$

In Ω, the roots of $S_n^{\pm}(\omega,\tau_1)$ are denoted as $\tau_1^{i\pm}, i = 1,2,\cdots$, and the corresponding τ_2 values are obtained

$$\tau_{2,i}^{j\pm}(\omega) = \frac{1}{\omega}[\arg(a_2(\omega,\tau_1^{i\pm})) - \omega\tau_1^{i\pm} \mp \theta_2(\omega,\tau_1^{i\pm}) + (2j+1)\pi]. \tag{3.19}$$

When ω takes all the values in the whole interval I_k, we have the following curve on Ω

$$C = \{(\omega,\tau_1^{i\pm}(\omega)) : \omega \in I_k, S_n^{\pm}(\omega,\tau_1^{i\pm}) = 0\}, \tag{3.20}$$

and the stability switching curves

$$\mathcal{T} = \{(\tau_1^{i\pm}(\omega),\tau_{2,i}^{j\pm}(\omega)) \in I \times \mathbb{R}_+ | \omega \in I_k, k = 1,2,\cdots,N\}. \tag{3.21}$$

3.2. Crossing direction

In this subsection, we consider the direction of $s(\tau_1,\tau_2)$ crossing the imaginary axis when (τ_1,τ_2) deviates from a crossing curve. Define the direction in which ω increases as the positive direction of the curve. As moving along the positive direction of the curve, the region on the left-hand (right-hand) side of the curve is called the region on the left (right).

Assume that $(\tau_1^*,\tau_2^*)\in\mathcal{T}$, then there is an $\omega^*>0$ such that $(\pm i\omega^*,\tau_1^*,\tau_2^*)$ is a pair of pure imaginary roots of Eq (3.2). If $\frac{\partial D}{\partial s}(iw^*,\tau_1^*,\tau_2^*)\neq 0$, then $s(\tau_1,\tau_2)=\mu(\tau_1,\tau_2)\pm i\omega(\tau_1,\tau_2)$ is a pair of conjugate complex roots of Eq (3.2), which satisfies $\mu(\tau_1^*,\tau_2^*)=0$ and $\omega(\tau_1^*,\tau_2^*)=\omega^*$ in the neighborhood of (τ_1^*,τ_2^*). Define the tangent vector of $\mathcal{T}$ along the positive direction as $\boldsymbol{n_1}=(\frac{\partial\tau_1}{\partial\omega},\frac{\partial\tau_2}{\partial\omega})$, and the normal vector to $\mathcal{T}$ pointing to the region on the right as $\boldsymbol{n_2}=(\frac{\partial\tau_2}{\partial\omega},-\frac{\partial\tau_1}{\partial\omega})$. When (τ_1,τ_2) moves along the direction $\boldsymbol{n_3}=(\frac{\partial\tau_1}{\partial\mu},\frac{\partial\tau_2}{\partial\mu})$, the direction in which the characteristic roots crossing the imaginary axis is determined by the sign of the inner product of $\boldsymbol{n_2}$ and $\boldsymbol{n_3}$. Let

$$\delta(\tau_1,\tau_2):=\boldsymbol{n_2}\cdot\boldsymbol{n_3}=(\frac{\partial\tau_2}{\partial\omega},-\frac{\partial\tau_1}{\partial\omega})\cdot(\frac{\partial\tau_1}{\partial\mu},\frac{\partial\tau_2}{\partial\mu})=\frac{\partial\tau_1}{\partial\mu}\frac{\partial\tau_2}{\partial\omega}-\frac{\partial\tau_2}{\partial\mu}\frac{\partial\tau_1}{\partial\omega}=\begin{vmatrix}\frac{\partial\tau_1}{\partial\mu} & \frac{\partial\tau_1}{\partial\omega}\\ \frac{\partial\tau_2}{\partial\mu} & \frac{\partial\tau_2}{\partial\omega}\end{vmatrix}.$$

Regarding τ_1 and τ_2 as a function of μ and ω at a neighborhood of $(0,\omega^*)$, and giving the following assumption

$$(H5)\quad det\begin{pmatrix}R_1(\tau_1^*,\tau_2^*) & R_2(\tau_1^*,\tau_2^*)\\ I_1(\tau_1^*,\tau_2^*) & I_2(\tau_1^*,\tau_2^*)\end{pmatrix}=R_1(\tau_1^*,\tau_2^*)I_2(\tau_1^*,\tau_2^*)-R_2(\tau_1^*,\tau_2^*)I_1(\tau_1^*,\tau_2^*)\neq 0,$$

by the implicit function theorem and $(H5)$, we have

$$\Delta(\tau_1^*,\tau_2^*):=\begin{pmatrix}\frac{\partial\tau_1^*}{\partial\mu} & \frac{\partial\tau_1^*}{\partial\omega}\\ \frac{\partial\tau_2^*}{\partial\mu} & \frac{\partial\tau_2^*}{\partial\omega}\end{pmatrix}\Bigg|_{\mu=0,\omega\in\Omega}=\begin{pmatrix}R_1(\tau_1^*,\tau_2^*) & R_2(\tau_1^*,\tau_2^*)\\ I_1(\tau_1^*,\tau_2^*) & I_2(\tau_1^*,\tau_2^*)\end{pmatrix}^{-1}\begin{pmatrix}R_0(\tau_1^*,\tau_2^*) & -I_0(\tau_1^*,\tau_2^*)\\ I_0(\tau_1^*,\tau_2^*) & R_0(\tau_1^*,\tau_2^*)\end{pmatrix},$$

where

$$\begin{aligned}R_0&=\frac{\partial ReD(s,\tau_1,\tau_2)}{\partial\mu}\Bigg|_{s=i\omega^*}\\
&=Re\Big\{P_0^{'}(i\omega^*,\tau_1^*)+(P_1^{'}(i\omega^*,\tau_1^*)-\tau_1^*P_1(i\omega^*,\tau_1^*))e^{-i\omega^*\tau_1^*}\\
&\quad+(P_2^{'}(i\omega^*,\tau_1^*)-(\tau_1^*+\tau_2^*)P_2(i\omega^*,\tau_1^*))e^{-i\omega^*(\tau_1^*+\tau_2^*)}\Big\}\\
&=P_0^{'R}+(P_1^{'R}-\tau_1^*P_1^R)\cos\omega^*\tau_1^*+(P_1^{'I}-\tau_1^*P_1^I)\sin\omega^*\tau_1^*\\
&\quad+(P_2^{'R}-(\tau_1^*+\tau_2^*)P_2^R)\cos\omega^*(\tau_1^*+\tau_2^*)+(P_2^{'I}-(\tau_1^*+\tau_2^*)P_2^I)\sin\omega^*(\tau_1^*+\tau_2^*)\\
&=4\theta\omega^{*4\theta-1}\sin 2\theta\pi+k\tau_1^*e^{-p\tau_1^*}\omega^{*3\theta}\cos(\frac{3\theta\pi}{2}-\omega^*\tau_1^*)+\omega^{*3\theta-1}[12\sigma\theta\sin\frac{3\theta\pi}{2}\\
&\quad-3k\theta e^{-p\tau_1^*}\sin(\frac{3\theta\pi}{2}-\omega^*\tau_1^*)]+\omega^{*2\theta}[3k\sigma\tau_1^*e^{-p\tau_1^*}\cos(\theta\pi-\omega^*\tau_1^*)\end{aligned}$$

$$
\begin{aligned}
&-(\tau_1^*+\tau_2^*)A_5\cos(\theta\pi-\omega^*(\tau_1^*+\tau_2^*))]+\omega^{*2\theta-1}[12\theta\sigma^2\sin\theta\pi\\
&-6k\theta\sigma e^{-p\tau_1^*}\sin(\theta\pi-\omega^*\tau_1^*)+2\theta A_5\sin(\theta\pi+\omega^*(\tau_1^*+\tau_2^*))]\\
&+\omega^{*\theta}[\tau_1^*e^{-p\tau_1^*}A_3\cos(\frac{\theta\pi}{2}-\omega^*\tau_1^*)-(\tau_1^*+\tau_2^*)A_6\cos(\frac{\theta\pi}{2}-\omega^*(\tau_1^*+\tau_2^*))]\\
&+\omega^{*\theta-1}[A_1\theta\sin\frac{\theta\pi}{2}-A_3\theta e^{-p\tau_1^*}\sin(\frac{\theta\pi}{2}-\omega^*\tau_1^*)+\theta A_6\sin(\frac{\theta\pi}{2}+\omega^*(\tau_1^*+\tau_2^*))]\\
&-(\tau_1^*+\tau_2^*)A_7\cos\omega^*(\tau_1^*+\tau_2^*),
\end{aligned}
$$

$$
\begin{aligned}
I_0 &= \frac{\partial ImD(s,\tau_1,\tau_2)}{\partial\mu}\Big|_{s=i\omega^*}\\
&= Im\Big\{P_0'(i\omega^*,\tau_1^*)+(P_1'(i\omega^*,\tau_1^*)-\tau_1^*P_1(i\omega^*,\tau_1^*))e^{-i\omega^*\tau_1^*}\\
&\quad+(P_2'(i\omega^*,\tau_1^*)-(\tau_1^*+\tau_2^*)P_2(i\omega^*,\tau_1^*))e^{-i\omega^*(\tau_1^*+\tau_2^*)}\Big\},\\
&= P_0'^I+(P_1'^I-\tau_1^*P_1^I)\cos\omega^*\tau_1^*-(P_1'^R-\tau_1^*P_1^R)\sin\omega^*\tau_1^*\\
&\quad+(P_2'^I-(\tau_1^*+\tau_2^*)P_2^I)\cos\omega^*(\tau_1^*+\tau_2^*)-(P_2'^R-(\tau_1^*+\tau_2^*)P_2^R)\sin\omega^*(\tau_1^*+\tau_2^*)\\
&= -4\theta\omega^{*4\theta-1}\cos2\theta\pi+k\tau_1^*e^{-p\tau_1^*}\omega^{*3\theta}\sin(\frac{3\theta\pi}{2}-\omega^*\tau_1^*)+\omega^{*3\theta-1}[-12\sigma\theta\cos\frac{3\theta\pi}{2}\\
&\quad+3k\theta e^{-p\tau_1^*}\cos(\frac{3\theta\pi}{2}-\omega^*\tau_1^*)]+\omega^{*2\theta}[3k\sigma\tau_1^*e^{-p\tau_1^*}\sin(\theta\pi-\omega^*\tau_1^*)\\
&\quad-(\tau_1^*+\tau_2^*)A_5\sin(\theta\pi-\omega^*(\tau_1^*+\tau_2^*))]+\omega^{*2\theta-1}[-12\theta\sigma^2\cos\theta\pi\\
&\quad+6k\theta\sigma e^{-p\tau_1^*}\cos(\theta\pi-\omega^*\tau_1^*)+2\theta A_5\cos(\theta\pi+\omega^*(\tau_1^*+\tau_2^*))]\\
&\quad+\omega^{*\theta}[\tau_1^*e^{-p\tau_1^*}A_3\sin(\frac{\theta\pi}{2}-\omega^*\tau_1^*)-(\tau_1^*+\tau_2^*)A_6\sin(\frac{\theta\pi}{2}-\omega^*(\tau_1^*+\tau_2^*))]\\
&\quad+\omega^{*\theta-1}[-A_1\theta\cos\frac{\theta\pi}{2}+A_3\theta e^{-p\tau_1^*}\cos(\frac{\theta\pi}{2}-\omega^*\tau_1^*)+\theta A_6\cos(\frac{\theta\pi}{2}+\omega^*(\tau_1^*+\tau_2^*))]\\
&\quad+(\tau_1^*+\tau_2^*)A_7\sin\omega^*(\tau_1^*+\tau_2^*),
\end{aligned}
$$

$$
\begin{aligned}
R_1 &= \frac{\partial ReD(s,\tau_1,\tau_2)}{\partial\tau_1}\Big|_{s=i\omega^*}\\
&= Re\Big\{P_{0\tau_1^*}'(i\omega^*,\tau_1^*)+P_{1\tau_1^*}'(i\omega^*,\tau_1^*)e^{-i\omega^*\tau_1^*}+P_{2\tau_1^*}'(i\omega^*,\tau_1^*)e^{-i\omega^*(\tau_1^*+\tau_2^*)}\\
&\quad-i\omega^*[P_1(i\omega^*,\tau_1^*)e^{-i\omega^*\tau_1^*}+P_2(i\omega^*,\tau_1^*)e^{-i\omega^*(\tau_1^*+\tau_2^*)}]\Big\}\\
&= pe^{-p\tau_1^*}(k\omega^{*3\theta}\cos(\frac{3\theta\pi}{2}-\omega^*\tau_1^*)+3k\theta\sigma\omega^{*2\theta}\cos(\theta\pi-\omega^*\tau_1^*)\\
&\quad+A_3\omega^{*\theta}\cos(\frac{\theta\pi}{2}-\omega^*\tau_1^*)+A_4\cos\omega^*\tau_1^*)+\omega^*[-e^{-p\tau_1^*}(k\omega^{*3\theta}\sin(\frac{3\theta\pi}{2}-\omega^*\tau_1^*)\\
&\quad+3k\theta\sigma\omega^{*2\theta}\sin(\theta\pi-\omega^*\tau_1^*)+A_3\omega^{*\theta}\sin(\frac{\theta\pi}{2}-\omega^*\tau_1^*)-A_4\sin\omega^*\tau_1^*)\\
&\quad+A_5\omega^{*2\theta}\sin(\theta\pi-\omega^*(\tau_1^*+\tau_2^*))+A_6\omega^{*\theta}\sin(\frac{\theta\pi}{2}-\omega^*(\tau_1^*+\tau_2^*))-A_7\sin\omega^*(\tau_1^*+\tau_2^*)],
\end{aligned}
$$

$$
\begin{aligned}
I_1 &= \frac{\partial ImD(s,\tau_1,\tau_2)}{\partial \tau_1}\Big|_{s=i\omega^*} \\
&= Im\Big\{P'_{0\tau_1^*}(i\omega^*,\tau_1^*) + P'_{1\tau_1^*}(i\omega^*,\tau_1^*)e^{-i\omega^*\tau_1^*} + P'_{2\tau_1^*}(i\omega^*,\tau_1^*)e^{-i\omega^*(\tau_1^*+\tau_2^*)} \\
&\quad - i\omega^*[P_1(i\omega^*,\tau_1^*)e^{-i\omega^*\tau_1^*} + P_2(i\omega^*,\tau_1^*)e^{-i\omega^*(\tau_1^*+\tau_2^*)}]\Big\} \\
&= pe^{-p\tau_1^*}(k\omega^{*3\theta}\sin(\frac{3\theta\pi}{2}-\omega^*\tau_1^*) + 3k\theta\sigma\omega^{*2\theta}\sin(\theta\pi-\omega^*\tau_1^*) \\
&\quad + A_3\omega^{*\theta}\sin(\frac{\theta\pi}{2}-\omega^*\tau_1^*) - A_4\sin\omega^*\tau_1^*) - \omega^*[e^{-p\tau_1^*}(k\omega^{*3\theta}\cos(\frac{3\theta\pi}{2}-\omega^*\tau_1^*) \\
&\quad + 3k\theta\sigma\omega^{*2\theta}\cos(\theta\pi-\omega^*\tau_1^*) + A_3\omega^{*\theta}\cos(\frac{\theta\pi}{2}-\omega^*\tau_1^*) + A_4\cos\omega^*\tau_1^*) \\
&\quad - A_5\omega^{*2\theta}\cos(\theta\pi-\omega^*(\tau_1^*+\tau_2^*)) - A_6\omega^{*\theta}\cos(\frac{\theta\pi}{2}-\omega^*(\tau_1^*+\tau_2^*)) - A_7\cos\omega^*(\tau_1^*+\tau_2^*)], \\
R_2 &= \frac{\partial ReD(s,\tau_1,\tau_2)}{\partial \tau_2}\Big|_{s=i\omega^*} \\
&= Re\Big\{P_2(i\omega^*,\tau_1^*)e^{-i\omega^*(\tau_1^*+\tau_2^*)}\cdot(-i\omega^*)\Big\} \\
&= \omega^*[A_5\omega^{*2\theta}\sin(\theta\pi-\omega^*(\tau_1^*+\tau_2^*)) + A_6\omega^{*\theta}\sin(\frac{\theta\pi}{2}-\omega^*(\tau_1^*+\tau_2^*)) - A_7\sin\omega^*(\tau_1^*+\tau_2^*)], \\
I_2 &= \frac{\partial ImD(s,\tau_1,\tau_2)}{\partial \tau_2}\Big|_{s=i\omega^*} \\
&= Im\Big\{P_2(i\omega^*,\tau_1^*)e^{-i\omega^*(\tau_1^*+\tau_2^*)}\cdot(-i\omega^*)\Big\} \\
&= -\omega^*[A_5\omega^{*2\theta}\cos(\theta\pi-\omega^*(\tau_1^*+\tau_2^*)) + A_6\omega^{*\theta}\cos(\frac{\theta\pi}{2}-\omega^*(\tau_1^*+\tau_2^*)) + A_7\cos\omega^*(\tau_1^*+\tau_2^*)].
\end{aligned}
$$

Let

$$\delta(\tau_1,\tau_2) = det(\Delta(\tau_1,\tau_2)) = \begin{vmatrix} R_1 & R_2 \\ I_1 & I_2 \end{vmatrix}^{-1} \begin{vmatrix} R_0 & -I_0 \\ I_0 & R_0 \end{vmatrix}. \tag{3.22}$$

Since $R_0^2 + I_0^2 \geq 0$, we have

$$sign(\delta(\tau_1^*,\tau_2^*)) = sign(R_1I_2 - R_2I_1).$$

If $sign(\delta(\tau_1^*,\tau_2^*)) > 0(< 0)$, then the pair of eigenvalues $\mu(\tau_1,\tau_2) \pm i\omega(\tau_1,\tau_2)$ of Eq (3.2) crosses the imaginary axis to the right (left)-hand region of the curves $\mathcal{T}$, when (τ_1,τ_2) moves along the positive direction of the crossing curves $\mathcal{T}$.

Based on the above discussion, the following theorem is given

Theorem 3.2. *If $sign(\delta(\tau_1^*,\tau_2^*)) > 0(< 0)$, then a pair of pure imaginary roots of the characteristic equation $D(s,\tau_1,\tau_2) = 0$ crosses the imaginary axis from left to right when (τ_1,τ_2) passes through the crossing curve to the right (left) region, where*

$$sign(\delta(\tau_1^*,\tau_2^*)) = sign\Big\{-Re\{[P_{0\tau_1}^*e^{i\omega^*(\tau_1^*+\tau_2^*)} + (P_{1\tau_1}^* - i\omega^*P_1^*)e^{i\omega^*\tau_2^*} + (P_{2\tau_1}^* - i\omega^*P_2^*)]\overline{P_2^*}\}\Big\},$$

where $P_i^* = P_i(i\omega^*,\tau_1^*)$ and $P_{i\tau_1}^* = \frac{\partial P_i}{\partial \tau_1}(i\omega^*,\tau_1^*), i = 0,1,2.$

Proof. Since

$$R_1(\tau_1^*,\tau_2^*)I_2(\tau_1^*,\tau_2^*)-R_2(\tau_1^*,\tau_2^*)I_1(\tau_1^*,\tau_2^*)=-Im\Big\{\frac{\partial D}{\partial\tau_1}(i\omega^*,\tau_1^*,\tau_2^*)\cdot\overline{\frac{\partial D}{\partial\tau_2}(i\omega^*,\tau_1^*,\tau_2^*)}\Big\}.$$

By direct calculation there is

$$\begin{aligned}&R_1(\tau_1^*,\tau_2^*)I_2(\tau_1^*,\tau_2^*)-R_2(\tau_1^*,\tau_2^*)I_1(\tau_1^*,\tau_2^*)\\&=-Im\Big\{\frac{\partial D}{\partial\tau_1}(i\omega^*,\tau_1^*,\tau_2^*)\cdot\overline{\frac{\partial D}{\partial\tau_2}(i\omega^*,\tau_1^*,\tau_2^*)}\Big\}\\&=-Im\Big\{\Big[P_{0\tau_1}^*+(P_{1\tau_1}^*-i\omega^*P_1^*)e^{-i\omega^*\tau_1^*}+(P_{2\tau_1}^*-i\omega^*P_2^*)e^{-i\omega^*(\tau_1^*+\tau_2^*)}\Big]\cdot\overline{(-i\omega^*)P_2^*e^{-i\omega^*(\tau_1^*+\tau_2^*)}}\Big\}\\&=-\omega^*Re\Big\{\Big[P_{0\tau_1}^*e^{i\omega^*(\tau_1^*+\tau_2^*)}+(P_{1\tau_1}^*-i\omega^*P_1^*)e^{i\omega^*\tau_2^*}+(P_{2\tau_1}^*-i\omega^*P_2^*)\Big]P_2^*\Big\},\end{aligned}$$

which completes the proof.

In the rest of this subsection, we further assume that
$(H6)$ $\quad \frac{\partial S_n^{\pm}(\omega,\tau_1)}{\partial\tau_1}\neq 0$, for any $(\tau_1,\tau_2)\in\mathcal{T}$.
To sum up, we have the the following theorem.

Theorem 3.3. *Assumptions* $(H1)$ *and* $(H4)-(H6)$ *hold.*
(i) *If* $(\tau_1,\tau_2)\in\mathcal{T}$, *then system* (1.2) *has a locally asymptotically stable equilibrium O ;*
(ii) *If* (τ_1,τ_2) *crosses the stability switching curves* $\mathcal{T}$, *then system* (1.2) *undergoes Hopf bifurcation at O.*

4. Numerical simulation

In this section, we consider the following system

$$\begin{cases}D^\theta x_1(t)=-1.1x_1(t)+0.5x_3(t)+1.3x_4(t-\tau_2),\\D^\theta x_2(t)=-1.1x_2(t)+1.3x_1(t)-x_4(t-\tau_2),\\D^\theta x_3(t)=-1.1x_3(t)+0.5x_2(t)-1.8x_4(t-\tau_2),\\D^\theta x_4(t)=-1.1x_4(t)-x_1(t-\tau_1)-x_2(t-\tau_1)+x_3(t-\tau_1)+ke^{-P(\tau_1)}x_4(t-\tau_1),\end{cases}\tag{4.1}$$

where $f(\cdot)=\tanh(\cdot),\theta=0.96$ and $P(\tau_1)=p\tau_1$. System (4.1) can be discussed in the following two cases.

Case I: $k=0$. Obviously, system (4.1) becomes uncontrolled system (1.1) when $k=0$. The characteristic equation corresponding to system (1.1) can be obtained

$$s^{4\theta}+4.4s^{3\theta}+7.26s^{2\theta}+4.99s^\theta+1.1066+(2.1s^{2\theta}+5.91s^\theta+1.695)e^{-s(\tau_1+\tau_2)}=0.$$

The relevant discussions are as follows.

1) When $\tau_1=0$ and $\tau_2=0$, it is easy to calculate that $D_1=4.4>0$, $D_2=30.275>0$ and $D_3=276.031>0$, $D_4=773.3284>0$. Therefore, it follows from Lemma 2.1 and Theorem 2.1 that the equilibrium O of system (4.1) is locally asymptotically stable (see Figure 1).

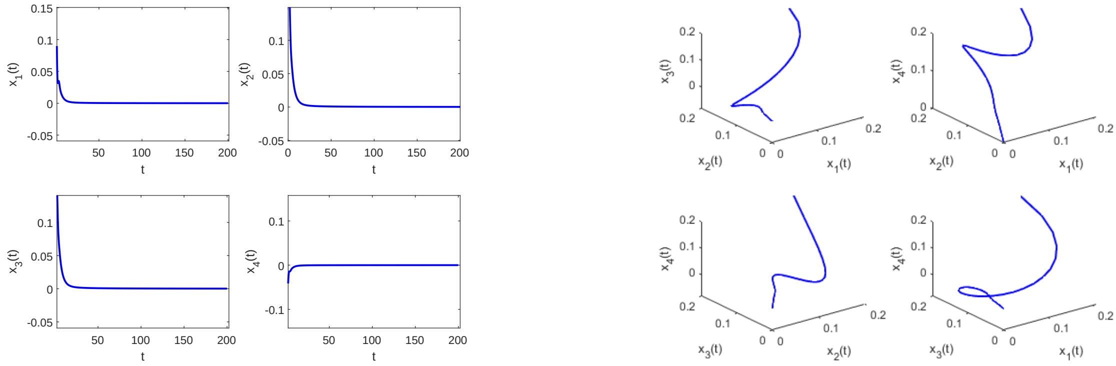

(a) (b)

Figure 1. The original equilibrium of system (4.1) with initial values (0.2, 0.2, 0.2, 0.2) is locally asymptotically stable when $\tau_1 = \tau_2 = 0$ and $k = 0$.

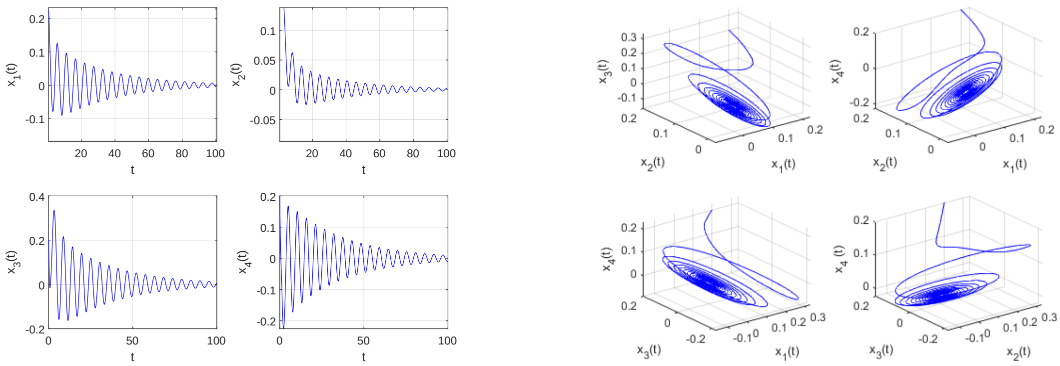

(a) (b)

Figure 2. The original equilibrium of system (4.1) with initial values (0.2, 0.2, 0.2, 0.2) is locally asymptotically stable when $\tau = 1.4 < \tau_0 = 1.5985$ and $k = 0$.

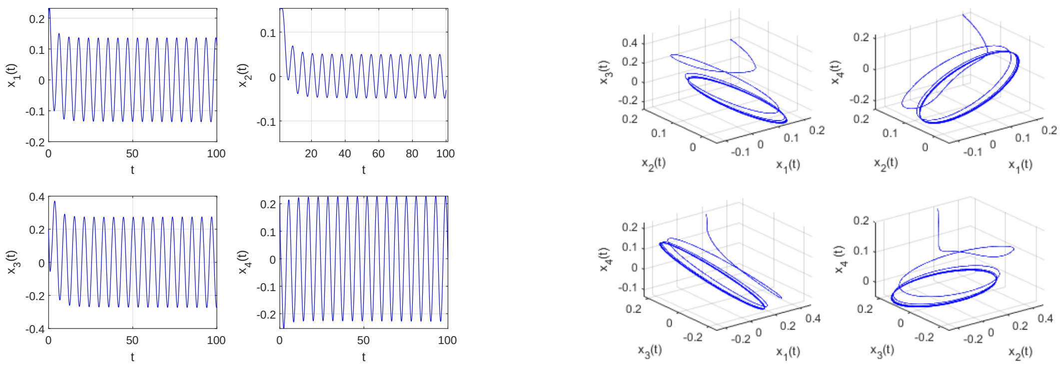

(a) (b)

Figure 3. System (4.1) with initial values (0.2, 0.2, 0.2, 0.2) undergoes Hopf bifurcation when $\tau = 1.6 > \tau_0 = 1.5985$ and $k = 0$.

2) When $\tau_1 > 0$ and $\tau_2 > 0$, from the definition of $F(\omega)$, we have

$$F(\omega) =\omega^{8\theta} + 0.5526\omega^{7\theta} + 4.954\omega^{6\theta} + 2.138\omega^{5\theta} + 6.797\omega^{4\theta} + 1.174\omega^{3\theta} - 18.82\omega^{2\theta} - 0.5633\omega^{\theta} - 1.648 = 0.$$

$c_8 = -1.648$, then $(H2)$ is satisfied. $\omega_0 = 1.079$ and $\tau_0 = 1.5985$ can be calculated from Eqs (2.8) and (2.9). According to the conditions of Theorem 2.2, it is also easy to validate that the equilibrium O of system (4.1) is locally asymptotically stable when $\tau = 1.4 < \tau_0$ (see Figure 2). System (4.1) exhibits Hopf bifurcation at the equilibrium O when $\tau = 1.6 > \tau_0$ (see Figure 3).

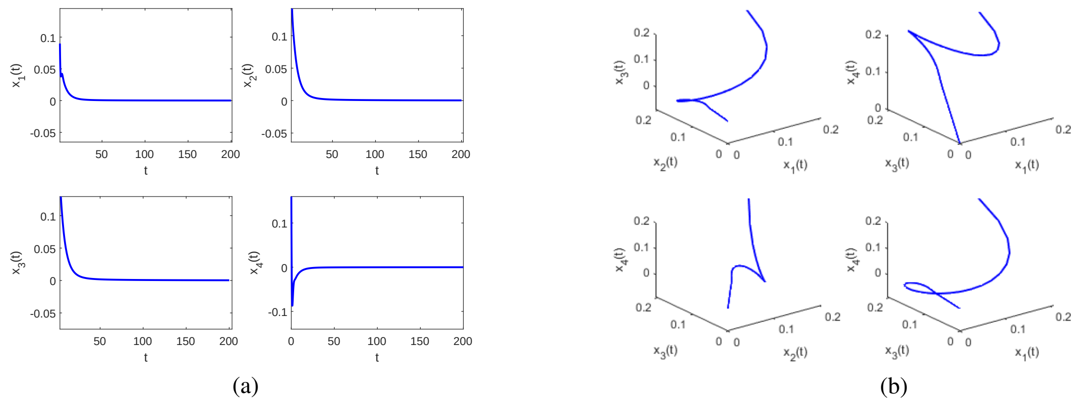

Figure 4. The original equilibrium of system (4.1) with initial values (0.2, 0.2, 0.2, 0.2) is locally asymptotically stable when $\tau_1 = \tau_2 = 0$ and $k = -0.5, p = 0.05$.

Case II: $k \neq 0$. System (4.1) corresponds to controlled system (1.2). Let $k = -0.5, p = 0.05$, the characteristic equation of system (1.2) can be obtained

$$P_0(s, \tau_1) + P_1(s, \tau_1)e^{-s\tau_1} + P_2(s, \tau_1)e^{-s(\tau_1+\tau_2)} = 0,$$

where

$$P_0(s, \tau_1) = s^{4\theta} + 4.4s^{3\theta} + 7.26s^{2\theta} + 4.999s^{\theta} + 1.1066,$$
$$P_1(s, \tau_1) = -e^{-0.05\tau_1}(-0.5s^{3\theta}-1.65s^{2\theta} - 1.815s^{\theta} - 0.308),$$
$$P_2(s, \tau_1) = 2.1s^{2\theta} + 5.91s^{\theta} + 1.695.$$

System (4.1) can be discussed in the following two cases.

1) When $\tau_1 = 0$ and $\tau_2 = 0$, we can calculate $B_4(B_1B_2B_3 - B_1^2B_4 - B_3^2) = 1398.964 > 0$, then $(H4)$ is satisfied. So the original equilibrium O is locally asymptotically stable from Theorem 3.1 (see Figure 4).

2) When $\tau_1 > 0, \tau_2 > 0$ and $\tau_1 \neq \tau_2$, the curves C and the feasible region Ω are shown in Figure 5. The curves C on Ω form stability switching curves $\mathcal{T}$ on (τ_1, τ_2) plane as in Figure 6(a). $sign(\delta(\tau_1^*, \tau_2^*)) = 1 > 0$ can be calculated, then the crossing direction of stability changes from left to right according to Theorem 3.2 (see Figure 6(a)). A partial enlargement is shown by the green area of Figure 6(a) (see Figure 6(b)). Choosing $(\tau_1, \tau_2) = (0.6, 1.5)$, we find that O is locally asymptotically

stable (see Figure 7). When (τ_1, τ_2) passes through stability switching curves from left to right along the arrow direction, by choosing $(\tau_1, \tau_2) = (0.65, 1.8)$, system (4.1) exhibits Hopf bifurcation at O (see Figure 8). When $(\tau_1, \tau_2) = (0.6, 1)$, the original equilibrium O of system (4.1) is locally asymptotically stable (see Figure 9). Compared with Figures 3 and 9, Hopf bifurcation of system with parameters delay feedback control could be delayed.

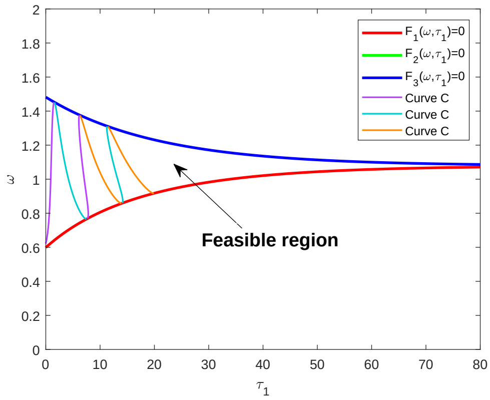

Figure 5. Graph of the feasible region Ω and C when $\tau_1 > 0, \tau_2 > 0$ and $k = -0.5, p = 0.05$.

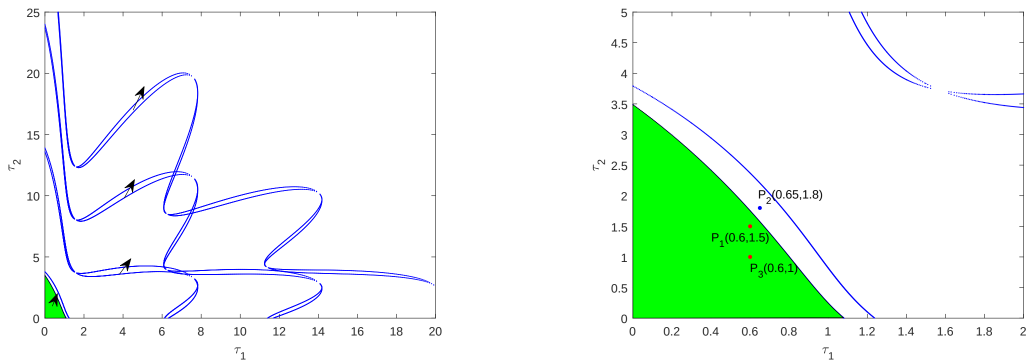

(a) (b)

Figure 6. (a) The stability switching curves of system (4.1) when $k = -0.5, p = 0.05$. (b) A partial enlargement of the green area of (a).

In order to highlight the control effect, we fix $p = 0.05, \theta = 0.96$ and take different parameter values for k to discuss. With the different values of $k = -0.5, -0.6, -0.7$, the corresponding stability switching curves are shown in Figure 10. In order to observe Figure 10 clearly, we give a partial enlargement of Figure 10. In particular, the region of the locally asymptotically stability of the equilibrium increases as k decreases when $p = 0.05, \theta = 0.96$ (see Figure 11). In addition, the influence of different fractional order values on the stability of system (4.1) is discussed as in Figure 12 when fixed $k = -0.5, p = 0.05$. When $\theta = 0.9, 0.96, 0.98$, its corresponding stability switching curves are shown in Figure 12, respectively. As can be seen from the partial enlargement of Figure 12, the region of the locally asymptotically stability of the equilibrium O decreases as θ increases when $k = -0.5, p = 0.05$ (see Figure 13). The results show that fractional order also can affect the stability of system.

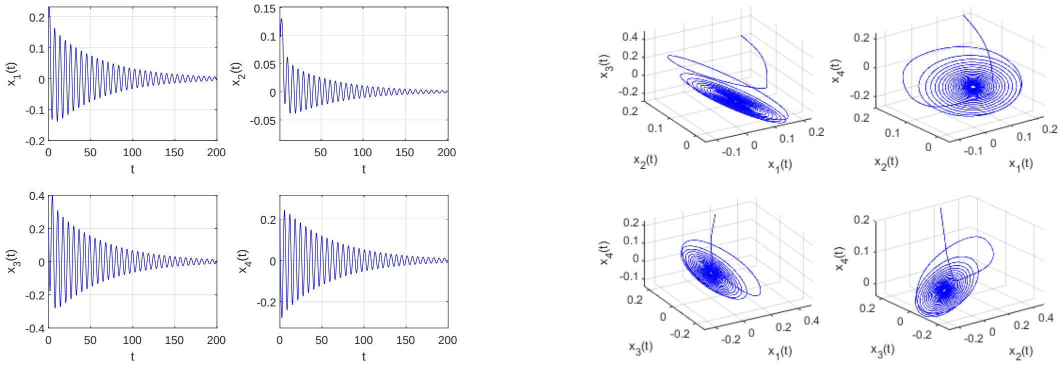

(a) (b)

Figure 7. The original equilibrium of system (4.1) with initial values $(0.2, 0.2, 0.2, 0.2)$ is locally asymptotically stable when $(\tau_1, \tau_2) = (0.6, 1.5)$ and $k = -0.5$, $p = 0.05$.

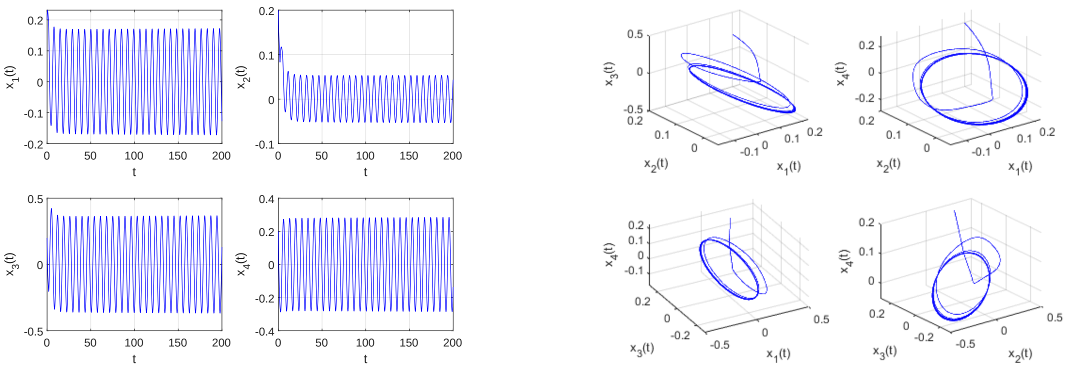

(a) (b)

Figure 8. The original equilibrium of system (4.1) with initial values $(0.2, 0.2, 0.2, 0.2)$ undergoes Hopf bifurcation when $(\tau_1, \tau_2) = (0.65, 1.8)$ and $k = -0.5$, $p = 0.05$.

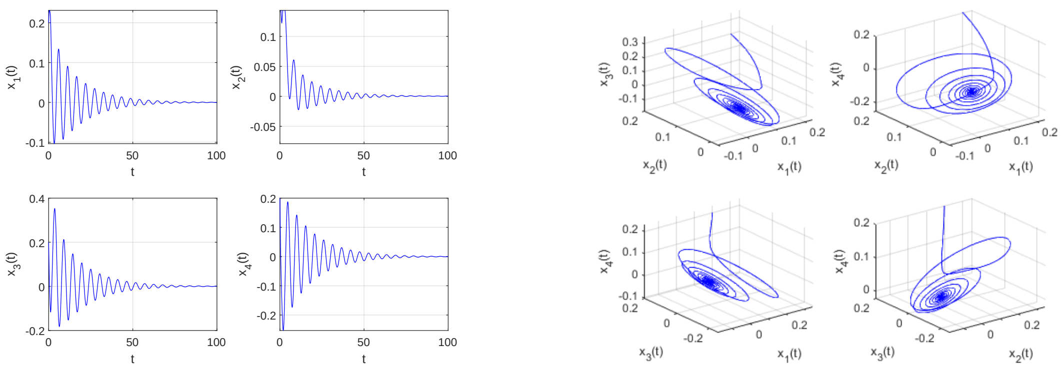

(a) (b)

Figure 9. The original equilibrium of system (4.1) with initial values $(0.2, 0.2, 0.2, 0.2)$ is locally asymptotically stable when $(\tau_1, \tau_2) = (0.6, 1)$ and $k = -0.5$, $p = 0.05$.

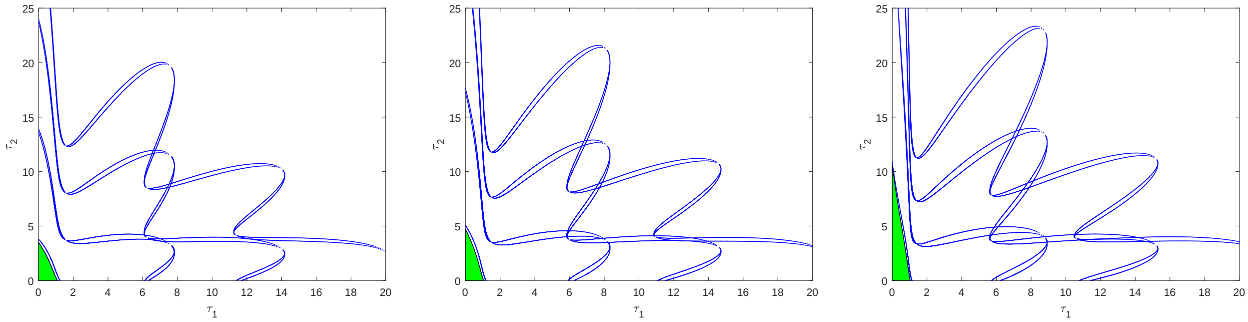

(a) $k = -0.5$ (b) $k = -0.6$ (c) $k = -0.7$

Figure 10. The stability switching curves of system (4.1) under different k when $p = 0.05, \theta = 0.96$.

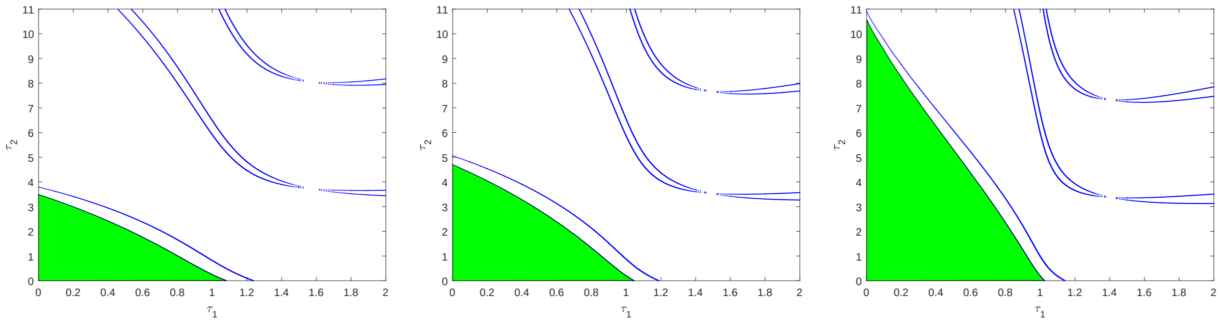

(a) $k = -0.5$ (b) $k = -0.6$ (c) $k = -0.7$

Figure 11. A partial enlargement of Figure 10.

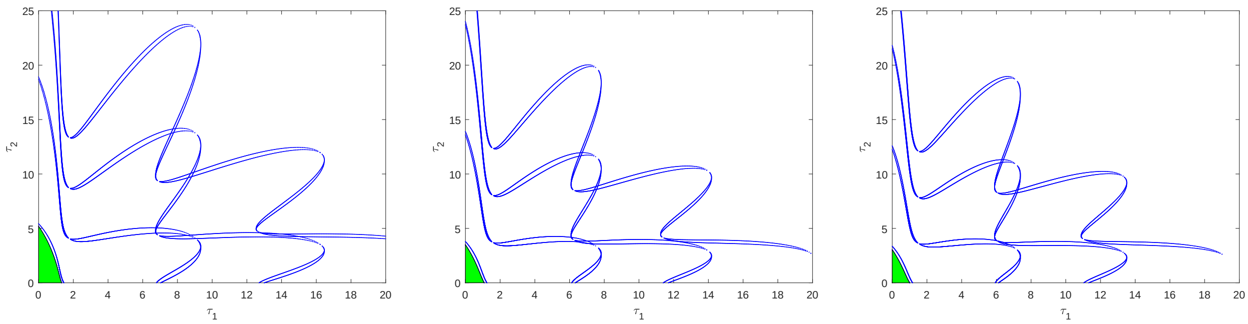

(a) $\theta = 0.9$ (b) $\theta = 0.96$ (c) $\theta = 0.98$

Figure 12. The stability switching curves of system (4.1) under different fractional orders when $k = -0.5, p = 0.05$.

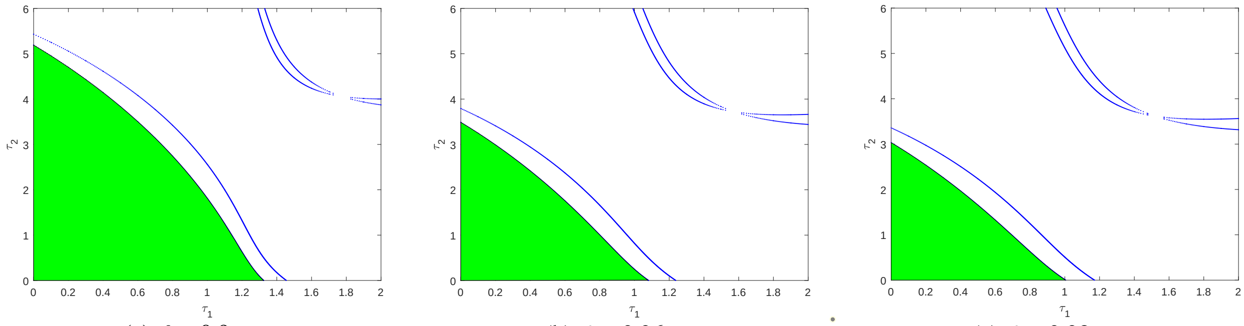

(a) $\theta = 0.9$ (b) $\theta = 0.96$ (c) $\theta = 0.98$

Figure 13. A partial enlargement of the green area of Figure 12.

5. Conclusions

In this paper, Hopf bifurcation control for a fractional-order two delays neural network with ring-hub structure has been studied. By selecting time delay as bifurcation parameters, the conditions for the local asymptotic stability of the equilibrium and the existence of Hopf bifurcation for uncontrolled system and controlled system are obtained respectively. In particular, the stability of system is discussed by the method of stability switching curves, and the region of the locally asymptotically stability of the equilibrium in (τ_1, τ_2) plane is obtained. The research results show that the introduction of parameters delay feedback controller can effectively control Hopf bifurcation of system. In addition, the influence of the change of control parameters on the stability of system are discussed. It is found that the region of the locally asymptotically stability at the equilibrium increases with the decrease of feedback control parameter k. When the other parameters remain unchanged, the region of the locally asymptotically stability at the equilibrium decreases as the increase of the order θ. Therefore, the stability of the equilibrium can be effectively improved by adjusting the feedback control parameters k and fractional-order θ. Our work has important significance for regulating the stability of network system performance. Especially in fields such as artificial intelligence, mechanical control, and image processing, our research can be applied in controlling Hopf bifurcation caused by time delays.

The characteristic equation of the following form is studied by using the method of stability switching curves in this paper:

$$P_0(s,\tau_1) + P_1(s,\tau_1)e^{-s\tau_1} + P_2(s,\tau_1)e^{-s(\tau_1+\tau_2)} = 0.$$

For fractional-order models with two delays and delay dependent parameters, the method of stability switching curves can also be applied to the following more general the characteristic equation

$$P_0(s,\tau_1) + P_1(s,\tau_1)e^{-s\tau_1} + P_2(s,\tau_1)e^{-s\tau_2} + P_3(s,\tau_1)e^{-s(\tau_1+\tau_2)} = 0. \tag{5.1}$$

However, since we need to consider a quadrilateral constructed by the four terms on the left hand side of Eq (5.1), the analysis of Eq (5.1) is more complicated and difficult.

Use of AI tools declaration

The authors declare they have not used Artificial Intelligence (AI) tools in the creation of this article.

Acknowledgments

This work was supported by the National Natural Science Foundation of China (No.11761040). We greatly appreciate the editors' and the anonymous referees' careful reading and helpful suggestions which have made the manuscript a real significant improvement.

Conflict of interest

All authors declare no conflicts of interest in this paper.

References

1. V. Perez-Munuzuri, V. Perez-Villar, L. Chua, Autowaves for image processing on a two-dimensional CNN array of excitable nonlinear circuits: flat and wrinkled labyrinths, *IEEE Trans. Circuits Syst. I: Fundam. Theory Appl.*, **40** (1993), 174–181. https://doi.org/10.1109/81.222798
2. L. Cheng, Z. Hou, Y. Lin, M. Tan, W. Zhang, F. Wu, Recurrent neural network for non-smooth convex optimization problems with application to the identification of genetic regulatory networks, *IEEE Trans. Neural Networks*, **22** (2011), 714–726. https://doi.org/10.1109/TNN.2011.2109735
3. Y. Sheng, Z. Zeng, T. Huang, Global stability of bidirectional associative memory neural networks with multiple time-varying delays, *IEEE Trans. Cybern.*, **52** (2020), 4095–4104. https://doi.org/10.1109/TCYB.2020.3011581
4. F. Hoppensteadt, E. Izhikevich, Pattern recognition via synchronization in phase-locked loop neural networks, *IEEE Trans. Neural Networks*, **11** (2000), 734–738. https://doi.org/10.1109/72.846744
5. M. Yang, X. Zhang, Y. Xia, Q. Liu, Q. Zhu, Adaptive neural network-based sliding mode control for a hydraulic rotary drive joint, *Comput. Electr. Eng.*, **102** (2022), 108189. https://doi.org/10.1016/j.compeleceng.2022.108189
6. C. Napoli, G. De Magistris, C. Ciancarelli, F. Corallo, F. Russo, D. Nardi, Exploiting Wavelet Recurrent Neural Networks for satellite telemetry data modeling, prediction and control, *Expert Syst. Appl.*, **206** (2022), 117831. https://doi.org/10.1016/j.eswa.2022.117831
7. H. Liang, Evaluation of fitness state of sports training based on self-organizing neural network, *Neural Comput. Appl.*, **33** (2021), 3953–3965. https://doi.org/10.1007/S00521-020-05551-W
8. R. Jia, Finite-time stability of a class of fuzzy cellular neural networks with multi-proportional delays, *Fuzzy Sets Syst.*, **319** (2017), 70–80. https://doi.org/10.1016/j.fss.2017.01.003
9. R. Rakkiyappan, J. Cao, G. Velmurugan, Existence and uniform stability analysis of fractional-order complex-valued neural networks with time delays, *IEEE Trans. Neural Networks Learn. Syst.* , **26** (2014), 84–97. https://doi.org/10.1109/TNNLS.2014.2311099
10. Y. Zheng, Delay-induced dynamical transitions in single Hindmarsh–Rose system, *Int. J. Bifurcation Chaos*, **23** (2013), 1350150. https://doi.org/10.1142/S0218127413501502
11. Y. Song, M. Han, J. Wei, Stability and Hopf bifurcation analysis on a simplified BAM neural network with delays, *Physica D*, **200** (2005), 185–204. https://doi.org/10.1016/j.physd.2004.10.010

12. Z. Wang, L. Li, Y. Li, Z. Cheng, Stability and Hopf bifurcation of a three-neuron network with multiple discrete and distributed delays, *Neural Process. Lett.*, **48** (2018), 1481–1502.

13. N. Ozcan, S. Arik, Global robust stability analysis of neural networks with multiple time delays, *IEEE Trans. Circuits Syst. I Regul. Pap.*, **53** (2006), 166–176. https://doi.org/10.1109/TCSI.2005.855724

14. S. Campbell, S. Ruan, G. Wolkowicz, J. Wu, Stability and bifurcation of a simple neural network with multiple time delays, *Fields Inst. Commun.*, **21** (1999), 65–79.

15. D. Baleanu, V. Balas, P. Agarwal, *Fractional Order Systems and Applications in Engineering*, Academic Press, 2023.

16. R. Hilfer, *Applications of Fractional Calculus in Physics*, World Scientific Publishing Company, 2000. https://doi.org/10.1142/3779

17. N. Tuan, H. Mohammadi, S. Rezapour, A mathematical model for COVID-19 transmission by using the Caputo fractional derivative, *Chaos*, **140** (2020), 110107. https://doi.org/10.1016/j.chaos.2020.110107

18. A. Bukhari, M. Raja, M. Sulaiman, S. Islam, M. Shoaib, P. Kumam, Fractional neuro-sequential ARFIMA-LSTM for financial market forecasting, *IEEE Access*, **8** (2020), 71326–71338.

19. C. Huang, H. Wang, J. Cao, Fractional order-induced bifurcations in a delayed neural network with three neurons, *Chaos Interdiscip. J. Nonlinear Sci.*, **33** (2023). https://doi.org/10.1063/5.0135232

20. C. Xu, Local and global Hopf bifurcation analysis on simplified bidirectional associative memory neural networks with multiple delays, *Math. Comput. Simul.*, **149** (2018), 69–90. https://doi.org/10.1016/j.matcom.2018.02.002

21. M. Xiao, W. Zheng, G. Jiang, J. Cao, Undamped oscillations generated by Hopf bifurcations in fractional-order recurrent neural networks with Caputo derivative, *IEEE Trans. Neural Networks Learn. Syst.*, **26** (2015), 3201–3214. https://doi.org/10.1109/TNNLS.2015.2425734

22. B. Tao, M. Xiao, W. Zheng, J. Cao, J. Tang, Dynamics analysis and design for a bidirectional super-ring-shaped neural network with n neurons and multiple delays, *IEEE Trans. Neural Networks Learn. Syst.*, **32** (2020), 2978–2992. https://doi.org/10.1109/TNNLS.2020.3009166

23. Y. Lu, M. Xiao, J. He, Z. Wang, Stability and bifurcation exploration of delayed neural networks with radial-ring configuration and bidirectional coupling, *IEEE Trans. Neural Networks Learn. Syst.*, **2023** (2023), 1–12. https://doi.org/10.1109/TNNLS.2023.3240403

24. J. Chen, M. Xiao, Y. Wan, C. Huang, F. Xu, Dynamical bifurcation for a class of large-scale fractional delayed neural networks with complex ring-hub structure and hybrid coupling, *IEEE Trans. Neural Networks Learn. Syst.*, **34** (2021), 2659–2669. https://doi.org/10.1109/TNNLS.2021.3107330

25. S. Ma, Q. Lu, Z. Feng, Double Hopf bifurcation for van der Pol-Duffing oscillator with parametric delay feedback control, *J. Math. Anal. Appl.*, **338** (2008), 993–1007. https://doi.org/10.1016/j.jmaa.2007.05.072

26. Z. Mao, H. Wang, D. Xu, Z. Cui, Bifurcation and hybrid control for a simple hopfield neural networks with delays, *Math. Prob. Eng.*, **2013** (2013). https://doi.org/10.1155/2013/315367

27. H. Zhao, W. Xie, Hopf bifurcation for a small-world network model with parameters delay feedback control, *Nonlinear Dyn.*, **63** (2011), 345–357. https://doi.org/10.1007/s11071-010-9808-1
28. Q. An, E. Beretta, Y. Kuang, C. Wang, H. Wang, Geometric stability switch criteria in delay differential equations with two delays and delay dependent parameters, *J. Differ. Equations*, **266** (2019), 7073–7100. https://doi.org/10.1016/j.jde.2018.11.025
29. D. Wang, Y. Liu, X. Gao, C. Wang, D. Fan, Dynamics of an HIV infection model with two time delays, *Discrete Contin. Dyn. Syst. Ser. B*, **28** (2023), 5641–5661. https://doi.org/10.3934/dcdsb.2023069
30. Z. Jiang, Y. Guo, Hopf bifurcation and stability crossing curve in a planktonic resource–consumer system with double delays, *Int. J. Bifurcation Chaos*, **30** (2020), 2050190. https://doi.org/10.1142/S0218127420501904
31. D. Matignon, Stability results for fractional differential equations with applications to control processing, *Comput. Eng. Syst. Appl.*, **2** (1996), 963–968.